This paper is available on line at http://www.mcponline.org

# SRC Homology 2 Domain-containing Leukocyte Phosphoprotein of 76 kDa (SLP-76) N-terminal Tyrosine Residues Regulate a Dynamic Signaling Equilibrium Involving Feedback of Proximal T-cell Receptor (TCR) Signaling*[S]

**Qinqin Ji‡, Yiyuan Ding‡, and Arthur R. Salomon‡§¶**

**SRC homology 2 domain-containing leukocyte phosphoprotein of 76 kDa (SLP-76) is a cytosolic adaptor protein that plays an important role in the T-cell receptor–mediated T-cell signaling pathway. SLP-76 links proximal receptor stimulation to downstream effectors through interaction with many signaling proteins. Previous studies showed that mutation of three tyrosine residues, $Tyr^{112}$, $Tyr^{128}$, and $Tyr^{145}$, in the N terminus of SLP-76 results in severely impaired phosphorylation and activation of Itk and PLC$\gamma$1, which leads to defective calcium mobilization, Erk activation, and NFAT activation. To expand our knowledge of the role of N-terminal phosphorylation of SLP-76 from these three tyrosine sites, we characterized nearly 1000 tyrosine phosphorylation sites via mass spectrometry in SLP-76 reconstituted wild-type cells and SLP-76 mutant cells in which three tyrosine residues were replaced with phenylalanines (Y3F mutant). Mutation of the three N-terminal tyrosine residues of SLP-76 phenocopied SLP-76-deficient cells for the majority of tyrosine phosphorylation sites observed, including feedback on proximal T-cell receptor signaling proteins. Meanwhile, reversed phosphorylation changes were observed on $Tyr^{192}$ of Lck when we compared mutants to the complete removal of SLP-76. In addition, N-terminal tyrosine sites of SLP-76 also perturbed phosphorylation of $Tyr^{440}$ of Fyn, $Tyr^{702}$ of PLC$\gamma$1, $Tyr^{204}$, $Tyr^{397}$, and $Tyr^{69}$ of ZAP-70, revealing new modes of regulation on these sites. All these findings confirmed the central role of N-terminal tyrosine sites of SLP-76 in the pathway and also shed light on novel signaling events that are uniquely regulated by SLP-76 N-terminal tyrosine residues.** ***Molecular & Cellular Proteomics 14: 10.1074/mcp.M114.037861, 30–40, 2015.***

Signaling events induced by the T-cell receptor (TCR)[1] play an essential role in the adaptive immune response, important for T-cell proliferation, differentiation, and cytokine secretion. TCR engagement results in sequential activation of Src kinase Lck and Fyn, which phosphorylates the CD3$\zeta$-chain immunoreceptor tyrosine-based activation motifs (ITAMs) (1). Phosphorylated ITAMs recruit and activate the Syk family protein kinase ZAP-70, which phosphorylates the transmembrane scaffold linker for activation of T cells (2), as well as SH2 domain-containing leukocyte protein of 76 kDa (SLP-76) (3), forming a signalosome complex essential for the assembly of downstream signaling proteins.

SLP-76, as an adaptor protein, lacks intrinsic enzymatic function but serves as an essential protein scaffold, recruiting other proteins for correct localization during T-cell signaling. Studies with SLP-76-deficient mice and SLP-76-deficient T-cell lines revealed a very profound role for SLP-76 in T-cell development and activation (4–7). In SLP-76-deficient Jurkat T cells, defects were observed in phosphorylation and activation of PLC$\gamma$1, calcium mobilization, Erk activation, and cytokine gene transcription following TCR ligation (6). SLP-76 consists of three domains: an N-terminal acidic region containing three tyrosine residues, Tyr112, Tyr128, and Tyr145; a central proline-rich region; and a C-terminal SH2 domain (7). Upon TCR activation, SLP-76 is recruited to the linker for activation of T cells signaling complex through binding with GADS (8), nucleating the interaction of signaling proteins, including PLC$\gamma$1, Itk, Vav, Nck, and adhesion and degranulation adaptor protein (9). PLC$\gamma$1 is recruited to the SLP-76

From the ‡Department of Chemistry, Brown University Providence, RI 02903; §Department of Molecular Biology, Cell Biology, and Biochemistry, Brown University Providence, RI 02903

Received January 14, 2014, and in revised form, July 31, 2014

Published, MCP Papers in Press, October 14, 2014, DOI 10.1074/mcp.M114.037861

Author contributions: Q.J. and A.R.S. designed research; Q.J. and Y.D. performed research; Q.J. analyzed data; Q.J. and A.R.S. wrote the paper.

[1] The abbreviations used are: TCR, T-cell receptor; Csk, C-terminal Src kinase; Erk, extracellular signal-regulated kinase; FDR, false discovery rate; Fyn, proto-oncogene tyrosine-protein kinase Fyn; ITAM, immunoreceptor tyrosine-based activation motif; Itk, interleukin 2–inducible T-cell kinase; Lck, lymphocyte-specific protein tyrosine kinase; PAG, phosphoprotein-associated glycolipid-enriched membrane protein; PLC$\gamma$, phospholipase C $\gamma$; SIC, select ion chromatogram; SILAC, stable isotope labeling of amino acids in cell culture; SLP-76, SH2 domain-containing leukocyte protein of 76 kDa; WT, wild type; ZAP-70, zeta-chain-associated protein kinase 70.

signaling complex through binding to both LAT and SLP-76. Phosphorylated $Tyr^{145}$ of SLP-76 is recognized by the SH2 domain of the Tec family kinase Itk, which also binds to the proline-rich domain of SLP-76 (10). This interaction maintains Itk in an active conformation (7). The binding of PLC$\gamma$ and active Itk to SLP-76 leads to the phosphorylation and activation of PLC$\gamma$1 and subsequent generation of the second messengers inositol 1,4,5-trisphosphate and diacylglcycerol (11). SLP-76 also regulates cytoskeletal rearrangement through the assembly of a tri-molecular signaling complex with Vav and Nck (12). In addition, the interaction between the tyrosine-phosphorylated adaptor protein and the SH2 domain of SLP-76 regulates integrin activation (13).

Besides its importance in regulating downstream signaling proteins, we recently revealed that SLP-76 plays an important role in mediating upstream signaling proteins (14). In a phosphoproteomic study examining cells deficient in SLP-76, SLP-76 was required for mediation of the phosphorylation of PAG (14), which transmits negative regulatory signals in complex with Csk (15). In addition, this earlier study revealed that the absence of SLP-76 perturbs the phosphorylation of Lck and, subsequently, a large number of Lck-regulated signaling molecules (*i.e.* CD3$\varepsilon$, -$\delta$, -$\gamma$, and -$\zeta$ chains; ZAP-70) (14). These findings led to the hypothesis that SLP-76 mediates both PAG negative feedback and ERK positive feedback of Lck (14).

Phosphorylation of three N-terminal tyrosine residues is essential for the function of SLP-76 (16). Upon phosphorylation by ZAP-70, phosphorylated $Tyr^{112}$ and $Tyr^{128}$ bind to SH2 domains of Vav (17–20), Nck (12, 21), and the p85 subunit of phosphatidylinositol 3-kinase (22), whereas phosphorylated $Tyr^{145}$ is recognized by the SH2 domain of Itk (10). N-terminal tyrosines of SLP-76 are required for the TCR-induced phosphorylation and activation of Itk and PLC$\gamma$1 (7).

However, the current understanding of N-terminal tyrosines of SLP-76 is incomplete, especially regarding their role in the newly discovered feedback regulation of the phosphorylation of upstream signaling proteins. For further elucidation of the function of SLP-76 N-terminal tyrosines in the regulation of the TCR signaling pathway, a wide-scale view of temporal changes in TCR signaling components is required. Quantitative mass-spectrometry-based phosphoproteomics is a powerful way to achieve this goal by enabling the system-wide identification of sites on proteins phosphorylated in the T cell, as well as the quantification of protein phosphorylation (14, 23–28). In this study, a wide-scale quantitative phosphoproteomic method was used to identify TCR-responsive tyrosine phosphorylation sites and to gain system-wide insight into the role of N-terminal tyrosine residues of SLP-76 in the TCR signaling pathway.

## EXPERIMENTAL PROCEDURES

*Cell Culture, SILAC Labeling, and T-cell Stimulation*—The SLP-76 mutant cell line J14–2D1 (also known as Y3F mutant) and its wild type (WT) SLP-76 reconstituted derivative J14–76-11 (6) were provided by Deborah Yablonski at Israel Institute of Technology. All cells were initially maintained in RPMI 1640 medium (Hyclone, Logan, UT) supplemented with 10% heat-inactivated undialyzed FBS (Hyclone), 2 mM L-glutamine, 100 U/ml penicillin G, and 100 $\mu$g/ml streptomycin (Invitrogen, Carlsbad, CA) in a humidified incubator with 5% $CO_2$ at 37 °C. SILAC was performed as described (25). Briefly, after 5 days, all cell lines were washed twice with RPMI 1640 medium without arginine and lysine (Invitrogen) and reconstituted in RPMI 1640 medium containing either $^{12}C_6$,$^{14}N_4$ arginine and $^{12}C_6$,$^{14}N_2$ lysine (Sigma) or $^{13}C_6$,$^{15}N_4$ arginine and $^{13}C_6$,$^{15}N_2$ lysine (Cambridge Isotope Laboratories, Andover, MA) supplemented with 10% heat-inactivated dialyzed FBS (Sigma), 2 mM L-glutamine, 100 U/ml penicillin G, 100 $\mu$g/ml streptomycin in a humidified incubator with 5% $CO_2$ at 37 °C for seven cell doublings. The concentrations of lysine and arginine used in SILAC labeling of Jurkat cells in experiments described here were 0.22 mM and 0.38 mM, respectively.

Anti-CD3 and anti-CD4 (clones OKT3 and OKT4, eBioscience, San Diego, CA) stimulation was performed as described (28). Briefly, cells were washed once with 4 °C PBS and reconstituted at a concentration of $1 \times 10^8$ cells/ml in PBS. For each time point, $1 \times 10^8$ cells were treated with OKT3 and OKT4 antibodies at a concentration of 2.5 $\mu$g/ml of each antibody for 10 min at 4 °C. Cells were then cross-linked with 22 $\mu$g/ml goat anti-mouse IgG (Jackson ImmunoResearch, West Grove, PA) and incubated at 37 °C for 0, 1, 1.5, 2, 3, 5, 7, or 10 min. To halt the stimulation, the 1-ml uncentrifuged cell suspension was lysed with the addition of 5 ml of lysis buffer (9 M urea, 1 mM sodium orthovanadate, and 20 mM HEPES, 2.5 mM sodium pyrophosphate, 1 mM $\beta$-glycerophosphate, pH 8.0), vortexed on a Vortex Mixer (Thermo Scientific) for 30 s, and then incubated for 20 min at 4 °C. Lysates were then sonicated at a 30-W output with two bursts of 30 s each and cleared at 12,000 $\times$ *g* for 15 min at 4 °C.

*Protein Reduction, Alkylation, Digestion, and Peptide Immunoprecipitation*—Protein concentrations were measured with the DC Protein Assay (Bio-Rad, Hercules, CA). Once protein concentrations were determined, a 5-mg equal portion of cell lysates from J14–2D1 and J14–76-11 was combined. The proteins in the lysate were reduced with 10 mM DTT for 20 min at 60 °C followed by alkylation with 100 mM iodoacetamide for 15 min at room temperature in the dark. Cell lysates were then diluted 4-fold with 20 mM HEPES buffer, pH 8.0, and digested with sequencing-grade modified trypsin (Promega, Madison, WI) in a 1:100 (w/w) trypsin:protein ratio overnight at room temperature. Tryptic peptides were acidified to pH 2.0 by the addition of 1/20 volume of 20% trifluoroacetic acid (TFA) for a final concentration of 1% TFA, cleared at 1800 $\times$ *g* for 5 min at room temperature, and desalted using C18 Sep-Pak plus cartridges (Waters, Milford, MA) as described (25), with the exception that TFA was used instead of acetic acid at the same required concentrations. Eluents containing peptides were lyophilized for 48 h to dryness.

Peptide immunoprecipitation was performed using p-Tyr-100 phosphotyrosine antibody beads (Cell Signaling Technology Danvers, MA). Dry peptides from each time point were reconstituted in ice-cold immunoaffinity purification buffer (5 mM MOPS, pH 7.2, 10 mM sodium phosphate, 50 mM NaCl) and further dissolved through gentle shaking for 30 min at room temperature and brief sonication in a sonicator water bath. Prior to peptide immunoprecipitation, a 10-pmol fraction of synthetic phosphopeptide LIEDAEpYTAK was added to each time-point sample as an exogenous quantitation standard. Peptide solutions were then cleared at 1800 $\times$ *g* for 5 min at room temperature, combined with p-Tyr-100 phosphotyrosine antibody beads, and incubated for 2 h at 4 °C. Beads were then washed three times with immunoaffinity purification buffer and twice with cold double-distilled $H_2O$ and eluted with 0.15% TFA. Eluted peptides were then desalted

using C18 Zip Tip pipette tips (Millipore Corporation, Billerica, MA) as described (29).

All phosphoproteomic data represent the average of five total replicate analyses for each time point.

*Automated Nano-LC/MS*—LC/MS was performed as described previously (25). Tryptic peptides were analyzed via a fully automated phosphoproteomic technology platform (30, 31). Phosphopeptides were eluted into an LTQ/Orbitrap Velos mass spectrometer (Thermo Fisher Scientific) through a PicoFrit analytical column (360-$\mu$m outer diameter, 75-$\mu$m inner diameter, fused-silica packed on a pressure bomb with 15 cm of 3-$\mu$m Monitor C18 particles; New Objective, Woburn, MA) with a reversed phase gradient (0% to 70% 0.1 M acetic acid in acetonitrile in 60 min, with a 90-min total method duration). An electrospray voltage of 1.8 kV was applied using a split flow configuration, as described previously (32). Spectra were collected in positive ion mode and in cycles of one full MS scan in the Orbitrap (*m/z*: 300–1700) followed by data-dependent MS/MS scans in the LTQ (~0.3 s each) sequentially of the 10 most abundant ions in each MS scan with charge state screening for +1, +2, and +3 ions and a dynamic exclusion time of 30 s. The automatic gain control was 1,000,000 for the Orbitrap scan and 10,000 for the LTQ scans. The maximum ion time was 100 ms for the LTQ scan and 500 ms for the Orbitrap full scan. The Orbitrap resolution was set at 60,000.

*Data Analysis*—MS/MS spectra were searched against the nonredundant human UniProt complete proteome set database containing 72,078 forward (UniProt database release 2011.10.21) and an equal number of reversed decoy protein entries using Mascot algorithm version 2.2.07 from Matrix Science (Boston MA) (33). Peak lists were generated using extractMSn version 5, provided by Thermo Fisher, using a mass range of 600–4500. The Mascot database search was performed with the following parameters: trypsin enzyme cleavage specificity, two possible missed cleavages, 7-ppm mass tolerance for precursor ions, and 0.5-Da mass tolerance for fragment ions. The search parameters specified differential modification of phosphorylation (+79.9663 Da) on serine, threonine, and tyrosine residues; dynamic modification of methionine oxidationn (+15.9949 Da); and static modification of carbamidomethylation (+57.0215 Da) on cysteine. The search parameters also included differential modification for arginine (+10.00827 Da) and lysine (+8.01420 Da) amino acids for the SILAC labeling. To provide high-confidence phosphopeptide sequence assignments, we filtered Mascot results by Mowse score (>20) and precursor mass error (<2 ppm). The resulting unique peptide assignments were filtered down to a 1% false discovery rate (FDR) using a logistic spectral score filter (34). The FDR was estimated with the decoy database approach after final assembly of non-redundant data into heatmaps (35). To validate the position of the phosphorylation sites, we applied the Ascore algorithm (36) to all data, and the reported phosphorylation site position reflected the top Ascore prediction.

*Quantitation of Relative Phosphopeptide Abundance*—Relative quantitation of phosphopeptide abundance was performed via calculation of select ion chromatogram (SIC) peak areas for heavy and light SILAC-labeled phosphopeptides. For label-free comparison of phosphopeptide abundance in SLP-76 reconstituted Jurkat cells among different time points of TCR stimulation, individual SIC peak areas were normalized to the peak area of an exogeneously spiked standard phosphopeptide, LIEDAEpYTAK. The LIEDAEpYTAK phosphopeptide was added in the same amount to every LC/MS sample and accompanied cellular phosphopeptides through peptide immunoprecipitation, desalting, and reversed-phase elution into the mass spectrometer. Retention time alignment of individual replicate analyses was performed as described previously (37). Peak areas were calculated through inspection of SICs using in-house software programmed in Microsoft Visual Basic 6.0 and based on Xcalibur Development Kit 2.1 (Thermo Fisher Scientific). This approach used the ICIS algorithm available in the Xcalibur XDK with the following parameters: multiple resolutions of 8, noise tolerance of 0.1, noise window of 40, scans in baseline of 5, and inclusion of refexc peaks parameter value, which is false. SIC peak areas were determined for every phosphopeptide that was identified by MS/MS. In the case of a missing MS/MS spectrum for a particular peptide in a particular replicate, peak areas were calculated according to the peptide's isolated mass and the retention time calculated from retention time alignment. A minimum SIC peak area equivalent to the typical spectral noise level of 300 was required of all data reported for label-free quantitation.

A label-free data heatmap was generated for the comparison of phosphopeptides in SLP-76 reconstituted cells through a time course of receptor stimulation as previously described (25). The magnitude of change of the heatmap color was calculated based on the natural log of the ratio of the fold change of each individual phosphopeptide peak area compared with the geometric mean for that phosphopeptide across all time points, as described previously (30). In the heatmap representation, the geometric mean of a given phosphopeptide across all time points was set to the color black. A blue color represented below-average abundance and yellow represented above-average abundance for each unique phosphopeptide. Blanks in the heatmap indicated that a clearly defined SIC peak was not observed for that phosphopeptide in any of the replicate analyses for that time point. The heatmap colors were generated from the average of the LIEDAEpYTAK standard phosphopeptide normalized SICs in the five replicate experiments. The coefficient of variation (cv) was calculated for each heatmap square. Label-free *p* values were calculated from the replicate data for each time point compared with the time point with the minimum average peak area for that phosphopeptide. *Q* values for multiple hypothesis tests were also calculated for each time point based on the determined *p* values using the R package QVALUE as previously described (38, 39). A white dot on a label-free heatmap square indicated that a significant difference ($Q$ value $< 0.05$) was detected for that phosphopeptide and time point relative to the time point with the minimal value.

In the second type of heatmap, SILAC ratios corresponding to phosphopeptide abundance differences between J14–2D1 and J14–76-11 cells across the time course of receptor stimulation were represented. For the SILAC heatmap, a black color represented a ratio of 1 between J14–2D1 and J14–76-11 for the peak area of a given phosphopeptide at that time point. A red color represented less abundance and green represented higher abundance of the given phosphopeptide in J14–2D1 relative to J14–76-11 cells. The magnitude of change of the heatmap color was calculated as described (25). *Q* values were also calculated between the J14–2D1 and J14–76-11 cell replicate measurements for each phosphopeptide and time point. A white dot on a heatmap square indicated that a significant change ($Q$ value $< 0.05$) was observed between the replicate data from the J14–2D1 and J14–76-11 samples for that time point and phosphopeptide.

*Western Blot Analysis*—Total cellular protein from 9 M urea cell lysates was diluted 1:1 with a 2× sample loading buffer (4% SDS, 125 mM Tris-HCl, pH 6.8, 20% v/v glycerol, 5% 2-mercaptoethanol, 0.01% bromphenol blue) for each proteomic sample. Equal amounts of protein, as measured by the DC Protein Assay, were separated via 4–20% SDS-PAGE on Precise Tris-HEPES gel (Thermo Fisher Scientific) and electroblotted onto an Immobilon membrane (Millipore). The membrane was blocked for 30 min in Odyssey blocking buffer at room temperature (Li-Cor, Lincoln, NE) and then incubated with the primary antibody diluted 1:1000 overnight at 4 °C. Primary antibodies used in this study were mouse monoclonal ANTI-FLAG® M2 antibody F3165 (Sigma-Aldrich), phospho-p44/42 MAPK (Erk1/2) (Thr202/

Tyr204) rabbit antibody (Cell Signaling Technology), p44/42 MAPK (Erk1/2) mouse antibody (Cell Signaling Technology), phospho-PLCγ1 (Tyr783) rabbit antibody (Cell Signaling Technology), and PLCγ1 rabbit antibody (Cell Signaling Technology). The membrane was washed four times for 5 min at room temperature in PBS/0.1% Tween-20. The membrane was then incubated with anti-mouse IgG (Li-Cor) or anti-rabbit IgG (Li-Cor) for 45 min in Odyssey blocking buffer at room temperature and washed three times for 5 min with PBS/0.1% Tween-20. Bands were visualized using an Odyssey Imaging System (Li-Cor).

## RESULTS

A quantitative phosphoproteomic analysis of TCR signaling was used to compare SLP-76 reconstituted Jurkat T cell line J14–76-11 and SLP-76 mutant cell line J14–2D1, in which three N-terminal tyrosine residues were replaced with phenylalanines (Y3F mutant). For each cell line, a receptor stimulation time course experiment including eight time points and five replicates was performed. The resulting phosphoproteomic data represent a wide-scale view of the temporal changes of tyrosine phosphorylation events following TCR stimulation in the presence of SLP-76 Y3F. In all, 934 unique tyrosine phosphorylation sites residing on 658 proteins were identified at a 1% FDR. The expression level of SLP-76 in the SLP-76 Y3F cells and reconstituted cells was tested via Western blot with an anti-Flag M2 antibody. Analysis of nine replicates showed no significant difference in the SLP-76 expression level in J14–76-11 (SLP-76 WT reconstituted) and J14–2D1 (SLP-76 Y3F mutant) (supplemental Fig. S1*A*).

*Phosphoproteomic Sample Quantitation and Statistical Analysis*—After processing of phosphoproteomic samples and generation of raw MS phosphopeptide identifications, high-quality sequence assignments were determined using stringent criteria as described in "Experimental Procedures." Relative quantitation of phosphopeptide abundance via calculation of SIC peak areas was performed for each phosphopeptide at each time point. Ratios were also calculated through comparison of the SIC peak area of a phosphopeptide from SLP-76 Y3F to SLP-76 WT cells at each time point. A total of five replicate experiments were performed, and SIC peak areas and heatmaps were generated from the average values. For each sequenced phosphopeptide, two different visual representations of quantitative data in the form of heatmaps were generated to reflect either label-free or SILAC ratio data. For label-free heatmaps, the fold change in phosphorylation for each identified phosphopeptide was compared across TCR stimulation time points in SLP-76 WT cells. For SILAC heatmaps, the fold change for each phosphopeptide peak area between SLP-76 Y3F and SLP-76 WT cells was compared. A complete list of sequence and phosphorylation site assignments of all identified phosphopeptides with corresponding SIC peak areas calculated either from MS/MS or accurate mass/aligned retention time and statistics can be found in supplemental Table S1. A complete list of tyrosine phosphorylated peptides with MOWSE scores $>$ 20 and mass error $<$ 2 ppm including reversed database hits from every replicate and time point of TCR stimulation are provided in supplemental Table S2. A summary of the number of unique tyrosine phosphorylated peptides and phosphorylation sites identified through the MS/MS database search at a 1% FDR in each replicate and time point can be found in supplemental Table S3. Phosphopeptide replicate SIC peak areas calculated directly from MS/MS-identified peptides or from peptides identified via accurate mass and retention time alignment showed a high degree of correlation (J14–76-11: $r = 0.872 \pm 0.006$ from MS/MS, $r = 0.794 \pm 0.011$ from retention time alignment; J14–2D1: $r = 0.880 \pm 0.006$ from MS/MS, $r = 0.791 \pm 0.012$ from retention time alignment) (supplemental Table S4). Supplemental Fig. S2 shows a pairwise comparison of replicate SIC peak areas from J14–76-11 at 0 min calculated using MS/MS retention times or retention times based on spectral alignment. Moreover, scatter plots comparing average SIC peak areas calculated from MS/MS retention times or retention time spectral alignment showed a high degree of correlation ($r = 0.914$) (supplemental Fig. S3). In all, a total of 2295 unique peptides containing 862 unique tyrosine phosphorylation sites on 659 proteins were identified at a 1% FDR after filtering and assembly, of which 1940 unique peptides containing 745 unique tyrosine phosphorylation sites on 555 proteins showed statistically significant changes between SLP-76 Y3F and SLP-76 WT cells ($Q$ value $<$ 0.05) and 1646 unique peptides containing 665 unique tyrosine phosphorylation sites on 482 proteins showed statistically significant TCR-responsive changes in SLP-76 reconstituted cells ($Q$ value $<$ 0.05). The mass spectrometry proteomics raw data and annoted MS/MS spectra for all post-translational modification containing peptides have been deposited to the ProteomeXchange (http://proteomecentral.proteomexchange.org) via the PRIDE partner repository (40) with the dataset identifier PXD001094. Annotated MS/MS spectra for all post-translational modification containing peptides from this study are also provided in supplemental Fig. S4.

*Phosphorylation of Canonical TCR Signaling Proteins*—Of the confidently identified phosphopeptides in the analysis, 140 tyrosine phosphorylation sites on 58 proteins were found within the subset of proteins annotated in KEGG as TCR signaling pathway proteins, of which 113 phosphorylation sites on 49 proteins showed a statistically significant change in relative abundance ($Q$ value $<$ 0.05) between SLP-76 Y3F and SLP-76 WT cells (Fig. 1 and Fig. 2). The SLP-76 Y3F mutant cells had constitutive decreases in phosphorylation on PLCγ1, PLCγ2, PAG, and SHP-1. Significantly decreased phosphorylation in the SLP-76 Y3F cells was observed at later time points on Erk1 at $Tyr^{204}$ and Erk2 at $Tyr^{187}$, whereas the changes at early time points were not statistically significant. The quantitative phosphoproteomic data for a selection of sites were confirmed by Western blot analysis (supplemental Figs. S1*B* and S1*C*). Phosphorylation was elevated at early time points and decreased at later time points in SLP-76 Y3F

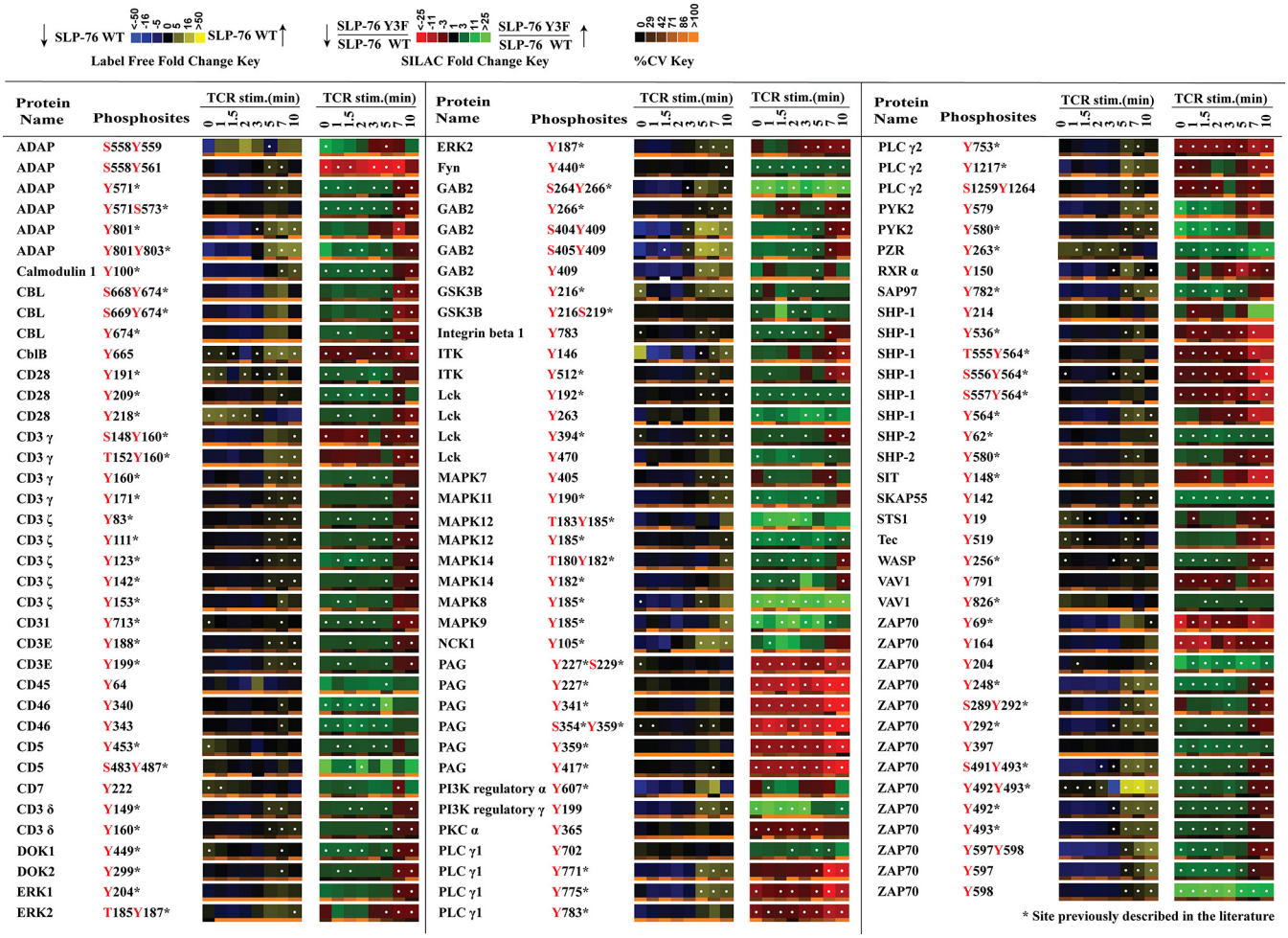


FIG. 1. **Quantitative phosphoproteomic analysis of known TCR signaling proteins.** Listed is a portion of the data collected representing proteins annotated in KEGG as T-cell receptor signaling proteins. Heatmaps were calculated from five replicate experiments. The label-free heatmap represents the temporal change in the phosphorylation of proteins from wild-type SLP-76 reconstituted cells (J14–76-11) through a time course of TCR stimulation. In the label-free heatmaps, black squares represent a phosphopeptide abundance equal to the geometric mean for that phosphopeptide across all time points. Yellow represents levels of phosphorylation above the average, and blue corresponds to less than average abundance (as indicated in the color legend). Within the label-free heatmap, white dots indicate a statistically significant difference ($Q$ value $< 0.05$) in the fold change in phosphopeptide abundance for that time point in the SLP-76 wild-type reconstituted cells. In the second SILAC heatmap, SILAC ratios between Y3F mutant cells (J14–2D1) and SLP-76 reconstituted cells (J14–76-11) are represented for each phosphopeptide at each time point according to the SILAC heatmap color key. Black signifies no change. Red represents reduced phosphorylation in Y3F mutant cells, and green represents elevated phosphorylation in Y3F mutant cells. White dots on SILAC heatmap squares indicate a statistically significant difference ($q$ value $< 0.05$) in the comparison between Y3F mutant and SLP-76 reconstituted cell SILAC ratios for that time point. Below each heatmap time point is a separate heatmap representing the coefficient of variation (cv) for that time point. According to the cv color key, black represents 0% cv, and more orange shading represents a greater cv. Blanks in the heatmaps indicate that a clearly defined SIC peak was not observed for that phosphopeptide at that time point.

cells on Lck, TCR proteins (CD3ε, -δ, -γ, and -ζ chains; ZAP-70), and other proteins (Itk, ADAP, DOK1, DOK2, PYK2). Furthermore, the temporal pattern of phosphorylation in Y3F relative to WT for a subset of sites diverged from the typical pattern of phosphorylation in other neighboring sites within the same protein. For example, Lck $Tyr^{192}$, Fyn $Tyr^{440}$, PLCγ1 $Tyr^{702}$, ZAP-70 $Tyr^{204}$, and $Tyr^{397}$ were all identified with elevated constitutive phosphorylation in SLP-76 Y3F cells, whereas ZAP-70 $Tyr^{69}$ was identified with constitutively decreased phosphorylation.

*Comparison of Effect in TCR Signaling Pathway between SLP-76-deficient (J14) and SLP-76 Y3F Cells*—To better understand the role of the N-terminal tyrosine sites of SLP-76 in the TCR signaling pathway, we compared phosphorylation changes of other signaling molecules between cells lacking SLP-76 protein and SLP-76 Y3F cells. A quantitative phosphoproteomic study of SLP-76-deficient and SLP-76 WT cells was performed in our lab and published recently. In that study, 74 tyrosine phosphorylation sites on 35 proteins within the KEGG T-cell signaling pathway were identified with sig-

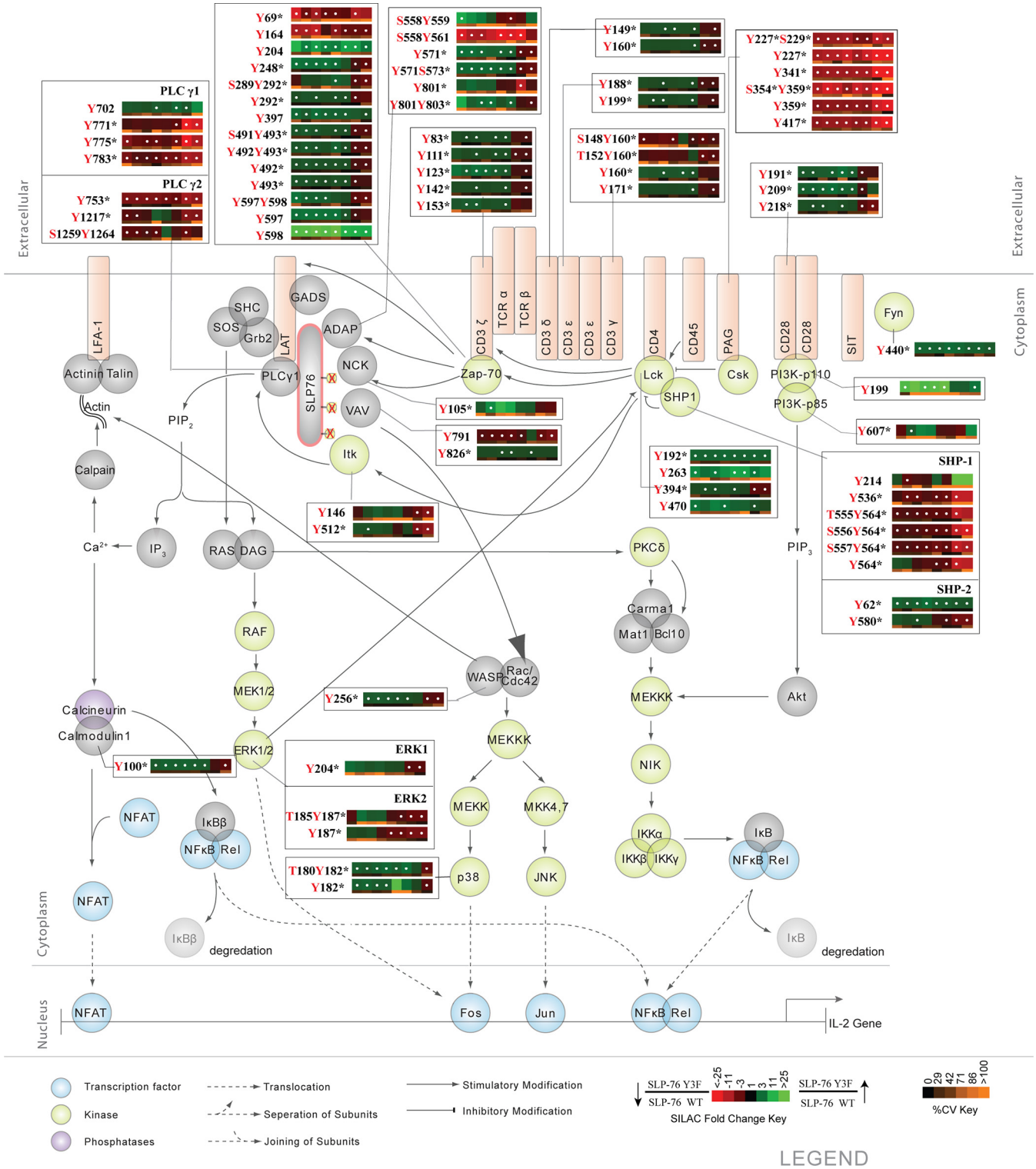


FIG. 2. **Effects of N-terminal tyrosine residues of SLP-76 on the canonical TCR signaling pathway.** The canonical T-cell signaling pathway is represented with SILAC heatmap quantitation and the corresponding identified phosphorylation sites. Heatmaps were calculated from the average of five replicate experiments. White dots within a heatmap square indicate a statistically significant difference ($Q$ value $< 0.05$) in the comparison between Y3F and SLP-76 reconstituted cells. SILAC heatmaps are described in detail in Fig. 1.

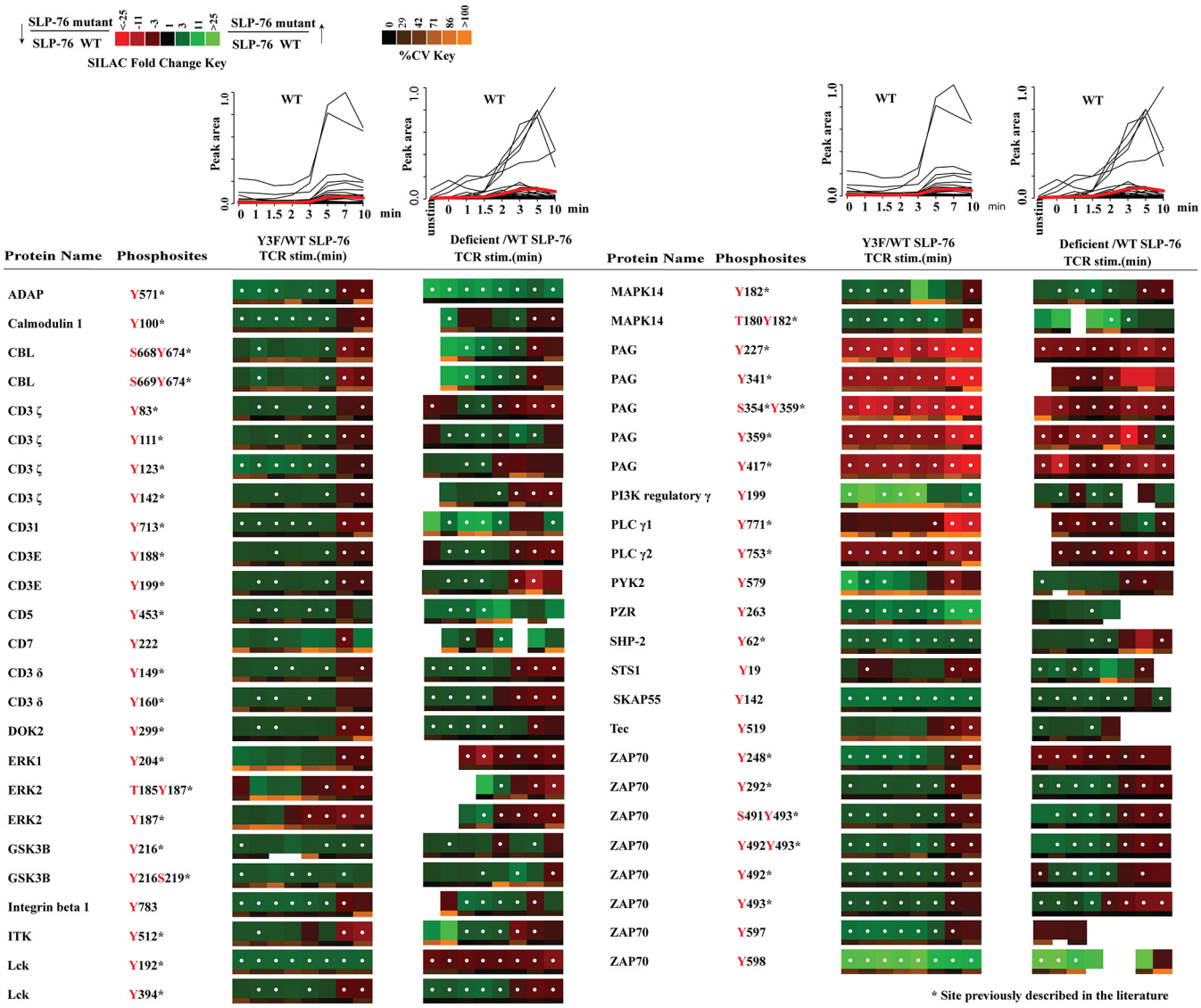


FIG. 3. **Quantitative phosphoproteomic analysis of known TCR signaling proteins identified in both this Y3F experiment and the previous SLP-76-deficient datasets.** SLP-76 reconstituted cells (WT) were used as a control in both studies. Line plots on top of the table represent the abundance of phosphopeptides observed from J14–76-11 (SLP-76 wild-type reconstituted cells) in either the Y3F study or the SLP-76-deficient cell study. Each black line represents one phosphopeptide, and the red line represents the average peak area of all the phosphopeptides in Fig. 3 at that time point. Heatmaps for Y3F experiments were calculated from the average of five replicate experiments, and heatmaps for J14 experiments were calculated from three replicate experiments. Green represents elevated phosphorylation in Y3F mutant cells or J14 cells relative to wild-type SLP-76 reconstituted cells, and red represents decreased phosphorylation. White dots within a heatmap square indicate a statistically significant difference ($Q$ value $< 0.05$) in the comparison between Y3F or SLP-76-deficient (J14) and SLP-76 reconstituted cells. The SILAC heatmaps are described in detail in Fig. 1.

nificant changes in relative abundance between SLP-76-deficient and SLP-76 WT cells (14). Among these sites, 49 tyrosine phosphorylation sites on 28 proteins were also identified with significant changes in relative abundance ($Q$ value $< 0.05$) between SLP-76 Y3F and SLP-76 WT cells in the present study. SLP-76 WT (J14–76-11) cells were used as the control cell line in both studies. Therefore, site-by-site comparison of SILAC heatmaps comparing the phosphorylation changes between SLP-76 mutant cells and SLP-76 WT cells will aid exploration of the function of SLP-76, especially the typical N-terminal tyrosine domain. The phosphorylation changes of these 49 tyrosine phosphorylation sites between the two studies were compared (Fig. 3). On top of each heatmap, the abundance of phosphopeptides from J14–76-11 cells (SLP-76 WT reconstituted) during the time course of T-cell stimulation is compared. The plots show some delay in the initiation of TCR signaling in the SLP-76 Y3F study relative to the SLP-76-deficient study. Despite this slight experimental variation in the timing of receptor stimulation, the phosphorylation of the majority of signaling proteins showed

the same phosphorylation change pattern when we compared the SLP-76-deficient and SLP-76 Y3F cells to the SLP-76 WT cells (Fig. 3). For example, a constitutive decrease in phosphorylation was observed on PLC$\gamma$1 Tyr$^{771}$, PLC$\gamma$2 Tyr$^{753}$ and PAG Tyr$^{227}$, Tyr$^{341}$, Ser$^{354}$Tyr$^{359}$, Tyr$^{359}$, Tyr$^{417}$. Also, a characteristic pattern with elevated phosphorylation at early time points and decreased phosphorylation at later time points was observed on Lck activation tyrosine residue Tyr$^{394}$ and many Lck-regulated proteins (CD3$\varepsilon$, -$\delta$, -$\gamma$, and -$\zeta$ chains; ZAP-70), as well as several other signaling proteins in both SLP-76 Y3F and SLP-76-deficient datasets. However, a divergent pattern was observed on Lck Tyr192 between these two studies.

## DISCUSSION

Tyrosine phosphorylation of three N-terminal tyrosine residues of SLP-76 is crucial for the function of SLP-76 (16). In this study, a quantitative mass-spectrometry-based phosphoproteomic strategy was utilized to study the systems-wide effects of phosphorylation of three N-terminal tyrosine residues of SLP-76 within TCR signaling.

*Itk May Phosphorylate PLC$\gamma$1 and PLC$\gamma$2 at Novel Sites*—Blocking the N-terminal phosphorylation of SLP-76 led to statistically significant decreases in the phosphorylation of Tyr$^{771}$, Tyr$^{775}$, and Tyr$^{783}$ of PLC$\gamma$1 and Tyr$^{753}$, Tyr$^{1217}$, and Tyr$^{1264}$ of PLC$\gamma$2 (Q value $<$ 0.05) (supplemental Figs. S5*B* and S5*C*). It is well established that Itk mediates the phosphorylation of PLC$\gamma$1 at Tyr$^{775}$ and Tyr$^{783}$ (7), two phosphorylation sites that are required for the activation of PLC$\gamma$1 (41). The binding of the SH2–SH3 domain of Itk with SLP-76 maintains Itk in an active formation (11). SLP-76, particularly its N-terminal tyrosine residues, is required for the activation of Itk as well as the phosphorylation of both PLC$\gamma$1 activation sites (7). Thus, the constitutively decreased phosphorylation of Tyr$^{775}$ and Tyr$^{783}$ on PLC$\gamma$1 is consistent with previous studies. The similar SILAC pattern of constitutively decreased phosphorylation on Tyr$^{771}$ suggests that this site might also be a substrate for Itk. PLC$\gamma$2 plays a crucial role in BCR-dependent calcium mobilization, and Tec-family kinases were demonstrated to phosphorylate PLC$\gamma$2 at Tyr$^{753}$ and Tyr$^{759}$, leading to PLC$\gamma$2-mediated calcium signaling (42). However, the study of the role of PLC$\gamma$2 in T cells is more limited. The constitutively decreased phosphorylation of PLC$\gamma$2 in Y3F cells suggests that Itk in T cells could also regulate PLC$\gamma$2 phosphorylation at Tyr$^{753}$, Tyr$^{1217}$, and Tyr$^{1264}$.

Impaired activation of PLC$\gamma$1 would lead to reduced production of the second messenger molecules inositol 1,4,5-trisphosphate and diacylglcycerol. Diacylglcycerol serves as a direct activator for Ras and PKC, leading to the activation of the Ras–Erk–AP1 and NF-$\kappa$B pathways, respectively (43). Erk2 activation was previously observed to be partially reduced in J14 (SLP-76 deficient cells) (6). Decreased phosphorylation of Tyr$^{204}$ of Erk1 and Tyr$^{187}$ of Erk2 was observed in SLP-76 Y3F cells relative to SLP-76 WT cells, as expected.

*SLP-76 Y3F Is Sufficient to Replicate the Majority of Phosphoproteome Changes Observed in SLP-76-deficient Cells*—With the advancement of instruments and methods, the number of tyrosine sites identified with statistically significant phosphorylation changes was improved almost 2-fold in this SLP-76 Y3F study relative to the previous SLP-76-deficient study. Nevertheless, among 47 tyrosine sites identified in both studies, the majority of them, especially 25 important tyrosine sites in the TCR signaling pathway, showed the same phosphorylation change pattern (Fig. 3). For example, decreased phosphorylation among the entire time course was observed in downstream tyrosine sites such as PLC$\gamma$1/2 and Erk 1/2 in both studies.

Constitutively decreased phosphorylation on Tyr$^{227}$, Tyr$^{341}$, Tyr$^{359}$, and Tyr$^{417}$ of PAG was observed in the SLP-76 Y3F study (supplemental Fig. S5*A*) and the previous SLP-76-deficient study. PAG is known to negatively regulate TCR signaling via recruitment of C-terminal Src kinase (Csk). Active Csk phosphorylates the C-terminal inhibitory tyrosine residues of Src-family kinases such as Lck and Fyn, down-regulating their kinase activities (15). In fact, the PAG–Csk complex represents a critical component of the negative homeostatic regulatory feedback mechanism restraining Lck activity (15). However, the regulation of phosphorylation of PAG is not well understood. Previous studies indicated that Fyn, but not Lck, is predominantly responsible for the phosphorylation of PAG in resting peripheral T cells (44). Interestingly, although one study suggested that CD45 phosphatase could act on Tyr$^{371}$ of PAG (45), another failed to confirm this finding (15). Our observation suggested that phosphorylation of the three N-terminal tyrosine residues of SLP-76 is required for the phosphorylation of PAG. One possible explanation for this observation is that phosphorylation of N-terminal tyrosine resides of SLP-76 is important in mediating the recruitment of Fyn to PAG. Another possibility is that phosphorylation of SLP-76 is required for the activity of Fyn or CD45.

Elevated phosphorylation at early time points and decreased phosphorylation at later time points was observed in the activation loop of Lck at Tyr$^{394}$ in the present SLP-76 Y3F study (supplemental Fig. S6*A*) and the previous SLP-76-deficient study. These findings reveal a previously undescribed regulatory network in which N-terminal tyrosine residues on SLP-76 are involved in both positive and negative feedback pathways that regulate the phosphorylation of the activation loop of Tyr$^{394}$ on Lck (14). Constitutively reduced phosphorylation on a variety of tyrosine residues on PAG in mutant cells would be expected to lead to a reduction in recruitment of the negative feedback regulator Csk, resulting in constitutively increased phosphorylation of Lck within its activation loop. Phosphorylation of Erk was increased with 5 to 10 min of TCR stimulation in cells reconstituted with WT SLP-76 (Fig. 1, label-free heatmap). We recently showed in Jurkat T cells (46), as others have shown in primary T cells (47), that inhibition of Erk activation leads to inhibition of positive feedback path-

ways through decreased phosphorylation of Ser$^{59}$ on Lck (48, 49). Our data support the hypothesis that N-terminal tyrosine residues of SLP-76 regulate competing negative feedback through Csk and positive feedback through Erk. According to this hypothesis, at early time points, Y3F SLP-76 mutant inhibition of PAG negative feedback outcompetes inhibition of Erk positive feedback because Erk is not robustly phosphorylated and activated. But at later time points when the phosphorylation and activation of Erk are much higher, inhibition of Erk positive feedback overcomes the inhibition of Csk negative feedback, leading to decreased phosphorylation at Lck Tyr$^{394}$ in the SLP-76 Y3F mutant.

Elevated phosphorylation at early time points and decreased phosphorylation in later time points was also observed on CD3$\varepsilon$, -$\delta$, -$\gamma$, and -$\zeta$ chains (supplemental Fig. S7) and ZAP-70 (supplemental Fig. S6*B*) in SLP-76 Y3F mutant cells. Phosphorylation of ITAM domains on the $\varepsilon$, $\delta$, $\gamma$, and $\zeta$ CD3 subunits by Lck is key to the initiation of signaling cascades that characterize T-cell activation (50–55). In Y3F mutant cells, elevated phosphorylation at early time points and decreased phosphorylation at later time points were observed on Tyr$^{149}$ and Tyr$^{160}$ of the CD3$\delta$ chain ($Q$ value $< 0.05$). A similar trend of phosphorylation change was also observed on CD3$\varepsilon$; Tyr$^{188}$ and Tyr$^{199}$, two sites known to be regulated by Lck (56); and Tyr$^{83}$, Tyr$^{111}$, Tyr$^{123}$, Tyr$^{142}$ of the CD3$\zeta$ chain. Besides the TCR ITAMs, a similar phosphorylation change pattern was also observed on Zap-70 Tyr$^{292}$, Tyr$^{492}$, and Tyr$^{493}$. It is well established that Lck mediates the phosphorylation of ZAP-70 at Tyr$^{493}$ to increase kinase activity of ZAP-70 in stimulated T cells (57). Autophosphorylation of both Tyr$^{292}$ and Tyr$^{492}$ on ZAP-70 is dependent on the initial phosphorylation of Tyr$^{493}$ (58).

Early increased and late decreased phosphorylation in the SLP-76 Y3F mutant was also observed on Tyr$^{512}$ of Itk (supplemental Fig. S6*C*). Itk is recruited to the cell membrane through the interaction of its pleckstrin homology domain with the membrane phosphatidylinositol 3,4,5-trisphosphate, where it becomes phosphorylated at Tyr$^{512}$ within its activation loop by Lck (59, 60). The TCR-induced global tyrosine phosphorylation of ITK was decreased in SLP-76-deficient T cells over the entire time course by immunoprecipitation of Itk from cell lysates followed by probe with pan-specific anti-phosphotyrosine (7). Nevertheless, this Western blot result did not measure phosphorylation at the specific site Tyr$^{512}$ of Itk, as the blot experiment was not site specific. In addition, our observation is consistent with the hypothesis of N-terminal tyrosine SLP-76-mediated competing positive and negative feedback pathways, as Itk is a known substrate of Lck (60). Taken together, these data suggest that SLP-76, especially its N-terminal tyrosine sites, regulates competing positive and negative feedback pathways that regulate not only Lck, but also its substrates (TCR ITAMs, ZAP-70, and Itk).

*Proline-rich Domain of SLP-76 Plays a Key Role in Phosphorylation of Lck Tyr$^{192}$*—Although the majority of sites responded similarly to the mutation of N-terminal tyrosine residues and to the complete removal of SLP-76, Lck Tyr$^{192}$ responded differently. Constitutively increased phosphorylation was observed in SLP-76 Y3F cells (supplemental Fig. S6*A*), compared with constitutively decreased phosphorylation in SLP-76-deficient cells. The difference in Lck Tyr$^{192}$ phosphorylation observed between mutant Y3F SLP-76 and SLP-76-deficient cells suggests that a domain of SLP-76 outside of the N-terminal tyrosine domain is regulating interaction between Lck and SLP-76. A previous study suggested that the interaction between Lck and SLP-76 is regulated by the interaction between the Lck SH3 domain and a proline-rich domain of SLP-76 outside of the N-terminal tyrosine domain (61). Our data, in combination with these previous data, support a new hypothesis that the regulation of Lck Tyr$^{192}$ but not Tyr$^{394}$ phosphorylation is independent of N-terminal tyrosine phosphorylation of SLP-76 and may be regulated by the interaction between Lck and the SLP-76 proline-rich domain.

*Acknowledgments*—We thank Dr. Deborah Yablonski at the Technician-Israel Institute of Technology for generously providing us with the Jurkat clones J14–2D1 (Y3F mutant cells) and J14-76-11 (SLP-76 reconstituted cells), and for the insightful discussions.

* This research is based in part upon work conducted using the Rhode Island NSF/EPSCoR Proteomics Share Resource Facility, which is supported in part by National Science Foundation EPSCoR Grant No. 1004057, National Institutes of Health Grant No. 1S10RR020923, a Rhode Island Science and Technology Advisory Council grant, and the Division of Biology and Medicine, Brown University. We acknowledge financial support from National Institutes of Health Grant No. R01AI083636.

S This article contains supplemental material.

¶ To whom correspondence should be addressed: Dr. Arthur R. Salomon, Tel.: 401-863-6091, Fax: 401-863-6087, E-mail: art@drsalomon.com.

REFERENCES

1. Zamoyska, R., Basson, A., Filby, A., Legname, G., Lovatt, M., and Seddon, B. (2003) The influence of the src-family kinases, Lck and Fyn, on T cell differentiation, survival and activation. *Immunol. Rev.* **191,** 107–118
2. Zhang, W., Sloan-Lancaster, J., Kitchen, J., Trible, R. P., and Samelson, L. E. (1998) LAT: the ZAP-70 tyrosine kinase substrate that links T cell receptor to cellular activation. *Cell* **92,** 83–92
3. Bubeck Wardenburg, J., Fu, C., Jackman, J. K., Flotow, H., Wilkinson, S. E., Williams, D. H., Johnson, R., Kong, G., Chan, A. C., and Findell, P. R. (1996) Phosphorylation of SLP-76 by the ZAP-70 protein-tyrosine kinase is required for T-cell receptor function. *J. Biol. Chem.* **271,** 19641–19644
4. Pivniouk, V., Tsitsikov, E., Swinton, P., Rathbun, G., Alt, F. W., and Geha, R. S. (1998) Impaired viability and profound block in thymocyte development in mice lacking the adaptor protein SLP-76. *Cell* **94,** 229–238
5. Clements, J. L., Yang, B., Ross-Barta, S. E., Eliason, S. L., Hrstka, R. F., Williamson, R. A., and Koretzky, G. A. (1998) Requirement for the leukocyte-specific adapter protein SLP-76 for normal T cell development. *Science* **281,** 416–419
6. Yablonski, D., Kuhne, M. R., Kadlecek, T., and Weiss, A. (1998) Uncoupling of nonreceptor tyrosine kinases from PLC-gamma 1 in an SLP-76-deficient T cell. *Science* **281,** 413–416
7. Bogin, Y., Ainey, C., Beach, D., and Yablonski, D. (2007) SLP-76 mediates and maintains activation of the Tec family kinase ITK via the T cell antigen receptor-induced association between SLP-76 and ITK. *Proc. Natl. Acad. Sci. U.S.A.* **104,** 6638–6643

8. Singer, A. L., Bunnell, S. C., Obstfeld, A. E., Jordan, M. S., Wu, J. N., Myung, P. S., Samelson, L. E., and Koretzky, G. A. (2004) Roles of the proline-rich domain in SLP-76 subcellular localization and T cell function. *J. Biol. Chem.* **279,** 15481–15490
9. Yablonski, D., and Weiss, A. (2001) Mechanisms of signaling by the hematopoietic-specific adaptor proteins, SLP-76 and LAT and their B cell counterpart, BLNK/SLP-65. *Adv. Immunol.* **79,** 93–128
10. Su, Y. W., Zhang, Y., Schweikert, J., Koretzky, G. A., Reth, M., and Wienands, J. (1999) Interaction of SLP adaptors with the SH2 domain of Tec family kinases. *Eur. J. Immunol.* **29,** 3702–3711
11. Qi, Q., and August, A. (2007) Keeping the (kinase) party going: SLP-76 and ITK dance to the beat. *Sci. STKE* **2007,** pe39
12. Bubeck Wardenburg, J., Pappu, R., Bu, J. Y., Mayer, B., Chernoff, J., Straus, D., and Chan, A. C. (1998) Regulation of PAK activation and the T cell cytoskeleton by the linker protein SLP-76. *Immunity* **9,** 607–616
13. Musci, M. A., Hendricks-Taylor, L. R., Motto, D. G., Paskind, M., Kamens, J., Turck, C. W., and Koretzky, G. A. (1997) Molecular cloning of SLAP-130, an SLP-76-associated substrate of the T cell antigen receptor-stimulated protein tyrosine kinases. *J. Biol. Chem.* **272,** 11674–11677
14. Cao, L., Ding, Y., Hung, N., Yu, K., Ritz, A., Raphael, B. J., and Salomon, A. R. (2012) Quantitative phosphoproteomics reveals SLP-76 dependent regulation of PAG and Src family kinases in T cells. *PLoS One* **7,** e46725
15. Brdicka, T., Pavlistova, D., Leo, A., Bruyns, E., Korinek, V., Angelisova, P., Scherer, J., Shevchenko, A., Hilgert, I., Cerny, J., Drbal, K., Kuramitsu, Y., Kornacker, B., Horejsi, V., and Schraven, B. (2000) Phosphoprotein associated with glycosphingolipid-enriched microdomains (PAG), a novel ubiquitously expressed transmembrane adaptor protein, binds the protein tyrosine kinase csk and is involved in regulation of T cell activation. *J. Exp. Med.* **191,** 1591–1604
16. Fang, N., Motto, D. G., Ross, S. E., and Koretzky, G. A. (1996) Tyrosines 113, 128, and 145 of SLP-76 are required for optimal augmentation of NFAT promoter activity. *J. Immunol.* **157,** 3769–3773
17. Raab, M., daSilva, A. J., Findell, P. R., and Rudd, C. E. (1997) Regulation of Vav-SLP-76 binding by ZAP-70 and its relevance to TCR zeta/CD3 induction of interleukin-2. *Immunity* **6,** 155–164
18. Onodera, H., Motto, D. G., Koretzky, G. A., and Rothstein, D. M. (1996) Differential regulation of activation-induced tyrosine phosphorylation and recruitment of SLP-76 to Vav by distinct isoforms of the CD45 protein-tyrosine phosphatase. *J. Biol. Chem.* **271,** 22225–22230
19. Tuosto, L., Michel, F., and Acuto, O. (1996) p95vav associates with tyrosine-phosphorylated SLP-76 in antigen-stimulated T cells. *J. Exp. Med.* **184,** 1161–1166
20. Wu, J., Motto, D. G., Koretzky, G. A., and Weiss, A. (1996) Vav and SLP-76 interact and functionally cooperate in IL-2 gene activation. *Immunity* **4,** 593–602
21. Wunderlich, L., Farago, A., Downward, J., and Buday, L. (1999) Association of Nck with tyrosine-phosphorylated SLP-76 in activated T lymphocytes. *Eur. J. Immunol.* **29,** 1068–1075
22. Shim, E. K., Moon, C. S., Lee, G. Y., Ha, Y. J., Chae, S. K., and Lee, J. R. (2004) Association of the Src homology 2 domain-containing leukocyte phosphoprotein of 76 kD (SLP-76) with the p85 subunit of phosphoinositide 3-kinase. *FEBS Lett.* **575,** 35–40
23. Mayya, V., Lundgren, D. H., Hwang, S. I., Rezaul, K., Wu, L. F., Eng, J. K., Rodionov, V., and Han, D. K. (2009) Quantitative phosphoproteomic analysis of T cell receptor signaling reveals system-wide modulation of protein-protein interactions. *Sci. Signal.* **2** p. ra46
24. Matsumoto, M., Oyamada, K., Takahashi, H., Sato, T., Hatakeyama, S., and Nakayama, K. I. (2009) Large-scale proteomic analysis of tyrosine-phosphorylation induced by T-cell receptor or B-cell receptor activation reveals new signaling pathways. *Proteomics* **9,** 3549–3563
25. Nguyen, V., Cao, L. L., Lin, J. T., Hung, N., Ritz, A., Yu, K. B., Jianu, R., Ulin, S. P., Raphael, B. J., Laidlaw, D. H., Brossay, L., and Salomon, A. R. (2009) A new approach for quantitative phosphoproteomic dissection of signaling pathways applied to T cell receptor activation. *Mol. Cell. Proteomics* **8,** 2418–2431
26. Kim, J. E., and White, F. M. (2006) Quantitative analysis of phosphotyrosine signaling networks triggered by CD3 and CD28 costimulation in Jurkat cells. *J. Immunol.* **176,** 2833–2843
27. Navarro, M. N., Goebel, J., Feijoo-Carnero, C., Morrice, N., and Cantrell, D. A. (2011) Phosphoproteomic analysis reveals an intrinsic pathway for the regulation of histone deacetylase 7 that controls the function of cytotoxic T lymphocytes. *Nat. Immunol.* **12,** 352–U111
28. Salomon, A. R., Ficarro, S. B., Brill, L. M., and Brinker, A. (2003) Profiling of tyrosine phosphorylation pathways in human cells using mass spectrometry. *Proc. Natl. Acad. Sci. U.S.A.* **100,** 443–448
29. Rappsilber, J., Ishihama, Y., and Mann, M. (2003) Stop and go extraction tips for matrix-assisted laser desorption/ionization, nanoelectrospray, and LC/MS sample pretreatment in proteomics. *Anal. Chem.* **75,** 663–670
30. Yu, K. B., and Salomon, A. R. (2009) PeptideDepot: flexible relational database for visual analysis of quantitative proteomic data and integration of existing protein information. *Proteomics* **9,** 5350–5358
31. Yu, K. B., and Salomon, A. R. (2010) HTAPP: high-throughput autonomous proteomic pipeline. *Proteomics* **10,** 2113–2122
32. Ficarro, S. B., Salomon, A. R., Brill, L. M., Mason, D. E., Stettler-Gill, M., Brock, A., and Peters, E. C. (2005) Automated immobilized metal affinity chromatography/nano-liquid chromatography/electrospray ionization mass spectrometry platform for profiling protein phosphorylation sites. *Rapid Commun. Mass Spectrom.* **19,** 57–71
33. Perkins, D. N., Pappin, D. J. C., Creasy, D. M., and Cottrell, J. S. (1999) Probability-based protein identification by searching sequence databases using mass spectrometry data. *Electrophoresis* **20,** 3551–3567
34. Yu, K. B., Sabelli, A., DeKeukelaere, L., Park, R., Sindi, S., Gatsonis, C. A., and Salomon, A. (2009) Integrated platform for manual and high-throughput statistical validation of tandem mass spectra. *Proteomics* **9,** 3115–3125
35. Elias, J. E., and Gygi, S. P. (2007) Target-decoy search strategy for increased confidence in large-scale protein identifications by mass spectrometry. *Nat. Methods* **4,** 207–214
36. Beausoleil, S. A., Villen, J., Gerber, S. A., Rush, J., and Gygi, S. P. (2006) A probability-based approach for high-throughput protein phosphorylation analysis and site localization. *Nat. Biotechnol.* **24,** 1285–1292
37. Demirkan, G., Yu, K., Boylan, J. M., Salomon, A. R., and Gruppuso, P. A. (2011) Phosphoproteomic profiling of in vivo signaling in liver by the mammalian target of rapamycin complex 1 (mTORC1). *PLoS One* **6,** e21729
38. Storey, J. D. (2003) The positive false discovery rate: a Bayesian interpretation and the q-value. *Ann. Stat.* **31,** 2013–2035
39. Storey, J. D., and Tibshirani, R. (2003) Statistical significance for genome-wide studies. *Proc. Natl. Acad. Sci. U.S.A.* **100,** 9440–9445
40. Vizcaino, J. A., Cote, R. G., Csordas, A., Dianes, J. A., Fabregat, A., Foster, J. M., Griss, J., Alpi, E., Birim, M., Contell, J., O'Kelly, G., Schoenegger, A., Ovelleiro, D., Perez-Riverol, Y., Reisinger, F., Rios, D., Wang, R., and Hermjakob, H. (2013) The PRoteomics IDEntifications (PRIDE) database and associated tools: status in 2013. *Nucleic Acids Res.* **41,** D1063–D1069
41. Serrano, C. J., Graham, L., DeBell, K., Rawat, R., Veri, M. C., Bonvini, E., Rellahan, B. L., and Reischl, I. G. (2005) A new tyrosine phosphorylation site in PLC gamma 1: the role of tyrosine 775 in immune receptor signaling. *J. Immunol.* **174,** 6233–6237
42. Humphries, L. A., Dangelmaier, C., Sommer, K., Kipp, K., Kato, R. M., Griffith, N., Bakman, I., Turk, C. W., Daniel, J. L., and Rawlings, D. J. (2004) Tec kinases mediate sustained calcium influx via site-specific tyrosine phosphorylation of the phospholipase C gamma Src homology 2-Src homology 3 linker. *J. Biol. Chem.* **279,** 37651–37661
43. Hickman, S. P., Yang, J., Thomas, R. M., Wells, A. D., and Turka, L. A. (2006) Defective activation of protein kinase C and Ras-ERK pathways limits IL-2 production and proliferation by CD4(+)CD25(+) regulatory T cells. *J. Immunol.* **177,** 2186–2194
44. Yasuda, K., Nagafuku, M., Shima, T., Okada, M., Yagi, T., Yamada, T., Minaki, Y., Kato, A., Tani-Ichi, S., Hamaoka, T., and Kosugi, A. (2002) Cutting edge: Fyn is essential for tyrosine phosphorylation of Csk-binding protein/phosphoprotein associated with glycolipid-enriched microdomains in lipid rafts in resting T cells. *J. Immunol.* **169,** 2813–2817
45. Davidson, D., Bakinowski, M., Thomas, M. L., Horejsi, V., and Veillette, A. (2003) Phosphorylation-dependent regulation of T-cell activation by PAG/Cbp, a lipid raft-associated transmembrane adaptor. *Mol. Cell. Biol.* **23,** 2017–2028
46. Helou, Y. A., Nguyen, V., Beik, S. P., and Salomon, A. R. (2013) ERK positive feedback regulates a widespread network of tyrosine phosphorylation sites across canonical T cell signaling and actin cytoskeletal proteins in Jurkat T cells. *PLoS One* **8,** e69641

47. Stefanova, I., Hemmer, B., Vergelli, M., Martin, R., Biddison, W. E., and Germain, R. N. (2003) TCR ligand discrimination is enforced by competing ERK positive and SHP-1 negative feedback pathways. *Nat. Immunol.* **4,** 248–254
48. Winkler, D. G., Park, I., Kim, T., Payne, N. S., Walsh, C. T., Strominger, J. L., and Shin, J. (1993) Phosphorylation of Ser-42 and Ser-59 in the N-terminal region of the tyrosine kinase p56lck. *Proc. Natl. Acad. Sci. U.S.A.* **90,** 5176–5180
49. Joung, I., Kim, T., Stolz, L. A., Payne, G., Winkler, D. G., Walsh, C. T., Strominger, J. L., and Shin, J. (1995) Modification of Ser59 in the unique N-terminal region of tyrosine kinase p56lck regulates specificity of its Src homology 2 domain. *Proc. Natl. Acad. Sci. U.S.A.* **92,** 5778–5782
50. Nika, K., Tautz, L., Arimura, Y., Vang, T., Williams, S., and Mustelin, T. (2007) A weak Lck tail bite is necessary for Lck function in T cell antigen receptor signaling. *J. Biol. Chem.* **282,** 36000–36009
51. Mustelin, T., Abraham, R. T., Rudd, C. E., Alonso, A., and Merlo, J. J. (2002) Protein tyrosine phosphorylation in T cell signaling. *Front. Biosci.* **7,** d918–d969
52. Straus, D. B., and Weiss, A. (1992) Genetic evidence for the involvement of the lck tyrosine kinase in signal transduction through the T cell antigen receptor. *Cell* **70,** 585–593
53. Samelson, L. E., Patel, M. D., Weissman, A. M., Harford, J. B., and Klausner, R. D. (1986) Antigen activation of murine T-cells induces tyrosine phosphorylation of a polypeptide associated with the T-cell antigen receptor. *Cell* **46,** 1083–1090
54. Baniyash, M., Garcia-Morales, P., Luong, E., Samelson, L. E., and Klausner, R. D. (1988) The T cell antigen receptor zeta chain is tyrosine phosphorylated upon activation. *J. Biol. Chem.* **263,** 18225–18230
55. Mustelin, T., and Altman, A. (1989) Do Cd4 and Cd8 control T-cell activation via a specific tyrosine protein-kinase. *Immunol. Today* **10,** 189–192
56. Guirado, M., de Aos, I., Orta, T., Rivas, L., Terhorst, C., Zubiaur, M., and Sancho, J. (2002) Phosphorylation of the N-terminal and C-terminal CD3-epsilon-ITAM tyrosines is differentially regulated in T cells. *Biochem. Biophys. Res. Commun.* **291,** 574–581
57. Chan, A. C., Dalton, M., Johnson, R., Kong, G. H., Wang, T., Thoma, R., and Kurosaki, T. (1995) Activation of Zap-70 kinase-activity by phosphorylation of tyrosine-493 is required for lymphocyte antigen receptor function. *EMBO J.* **14,** 2499–2508
58. Kong, G. H., Dalton, M., Wardenburg, J. B., Straus, D., Kurosaki, T., and Chan, A. C. (1996) Distinct tyrosine phosphorylation sites in ZAP-70 mediate activation and negative regulation of antigen receptor function. *Mol. Cell. Biol.* **16,** 5026–5035
59. August, A., Sadra, A., Dupont, B., and Hanafusa, H. (1997) Src-induced activation of inducible T cell kinase (ITK) requires phosphatidylinositol 3-kinase activity and the pleckstrin homology domain of inducible T cell kinase. *Proc. Natl. Acad. Sci. U.S.A.* **94,** 11227–11232
60. Heyeck, S. D., Wilcox, H. M., Bunnell, S. C., and Berg, L. J. (1997) Lck phosphorylates the activation loop tyrosine of the Itk kinase domain and activates Itk kinase activity. *J. Biol. Chem.* **272,** 25401–25408
61. Sanzenbacher, R., Kabelitz, D., and Janssen, O. (1999) SLP-76 binding to p56lck: a role for SLP-76 in CD4-induced desensitization of the TCR/CD3 signaling complex. *J. Immunol.* **163,** 3143–3152